doi.org/10.36721/PJPS.2025.38.6.REG.13739.1

Dual regulatory effects of Sheng-Di-Da-Huang decoction on microglial cells in rat models of intracerebral hemorrhage

Min Cai[1], Jingsi Zhang[2], Min Li[3], Li Yang[4], Jun Xiang[1], Xiangting Li[1], Yijin Xiang[1], Feng Yang[1], Wen Zhu[1], Xuxia Bao[1], Dongze Qiu[1], Wen Zhang[1] and Dingfang Cai[1]*

[1]Department of Integrative Medicine, Zhongshan Hospital and Laboratory of Neurology, Institute of Integrative Medicine, Fudan University, Shanghai, China
[2]Department of Neurology, Shuguang Hospital Affiliated to Shanghai University of Traditional Chinese Medicine, Shanghai, China
[3]Department of Ophthalmology, Zhongshan Hospital, Fudan University, Shanghai, China
[4]Department of Radiology, Zhongshan Hospital, Fudan University, Shanghai, China

Abstract: Two microglia phenotypes, M1 pro-inflammatory and M2 anti-inflammatory phenotypes, exert distinct functions post-intracerebral hemorrhage (post-IH). The M1-to-M2 switch is noted within 7 days, but precise timing remains undetermined. This research sought to examine the specific timing of the M1-to-M2 transition and examine the effect of Sheng-Di-Da-Huang Decoction (SDDHD) on M2 microglia post-IH. Rats were grouped into sham, IH and dose-varied SDDHD treatment cohorts. Rats of IH group had an intrastriatum injection of collagenase IV (0.2 U), while those of sham group were only injected with saline. All rats underwent neurological score assessment and magnetic resonance imaging (MRI) scans at different time points after procedure. The expression markers (iNOS for M1; Arg1, IL-4, and IL-10 for M2) were assessed across days. M1 markers (iNOS) peaked at day 3, whereas M2 markers (Arg1, IL-4 and IL-10) rose progressively, suggesting the M1-to-M2 switch around day 3. SDDHD decreased iNOS expression and elevated Arg1, IL-4 and IL-10 expression, improving neurological outcomes. SDDHD exhibits a bidirectional regulation of microglia, promoting M2 transformation while inhibiting M1, thereby enhancing neurological recovery post-IH.

Keywords: Intracerebral hemorrhage; M1 marker; M2 marker: Microglia; Sheng-Di-Da-Huang Decoction

Submitted on 20-11-2024 – Revised on 18-12-2024 – Accepted on 18-12-2024

INTRODUCTION

The latest research shows that stroke is the primary contributor to mortality in China (Zhou M *et al*., 2019). Intracerebral hemorrhage (IH), a nontraumatic rupture of a brain vessel, causes blood to accumulate in the brain. In Asia, IH is responsible for 20% to 30% of the global total of 15 million stroke cases (Puy *et al*., 2023). The proportion in China is higher, accounting for 18.8%-47.6% of all strokes (Wu *et al*., 2019). IH carries a 30-day mortality rate of around 40% (O'Carroll *et al*., 2021) and it always leaves the survivors severe neurological defects. Upon six months, only about 20% of sufferers are able to function independently (Fogelholm *et al*., 2005). Many efforts have been made to improve the situation, but over the past 40 years, the IH incidence has exhibited no obvious alteration (van Asch *et al*., 2010).

Neuroinflammation is crucial for brain injury recovery upon stroking, with microglia/macrophages acting as the primary executor. Microglia exhibit two identified phenotypes: The nociceptive/toxic M1 phenotype and the protective, reparative M2 phenotype. The M1 phenotype is known to produce proinflammatory cytokines, incorporating interleukin (IL)-1β, -12, -23 and tumor necrosis factor (TNF)-α, chemokines, reactive oxygen species and nitric oxide (NO), all of which encourage the breakdown of the blood-brain barrier (Mracsko and Veltkamp 2014; Kanazawa *et al*., 2017). CD16, CD86, inducible nitric oxide synthase (iNOS), and major histocompatibility complex (MHC) II are among the macrophage markers they express (Chowdhury and Trivedi 2023). Known for its anti-inflammatory properties, the M2 phenotype participates in trophic factor release, phagocytosis, tissue regeneration and inflammation resolution (Zhao *et al*., 2015). Cytokine IL-4, displaying anti-inflammatory features, induces M2 polarization, encouraging IL-10 production and elevating surface phenotype markers CD36, Ym-1, CD206 and arginase-1 (Arg-1) (Zhao *et al*., 2015).

A shift from M1 to M2 phenotype occurs in the first 7 days following IH, although the timing and mechanisms behind this change keep uncertain (Zhao *et al*., 2015). Our prior research confirmed that the pro-inflammatory functions of microglia peaked at 3 days and then gradually decreased. Sheng-Di-Da-Huang Decoction (SDDHD) decreased the inflammatory response by inhibiting the activation of microglia (Cai *et al*., 2018). This investigation focused on researching the specific timing of the transformation of M1-to-M2 phenotype microglia based on their associated markers changes over time upon IH, and how SDDHD influenced M2 phenotype microglia.

**Corresponding author:* e-mail: dingfangcai@163.com

MATERIALS AND METHODS

Animals and IH model

Rats of the Sprague-Dawley strain, male and with a weight range of 300–350 g, were recruited. As described in earlier work, ICHIH model induction was achieved via intrastriatal collagenase IV administration (Cai *et al*., 2018). Briefly, after anesthesia employing intraperitoneal pentobarbital (40 mg/kg), rats were positioned within a stereotaxic apparatus (David Kopf Instruments, Tujunga, CA). One hole was drilled located 3 mm lateral and 0.2 mm anterior to bregma, extending to a 6 mm depth. Collagenase IV (1 microliter, 0.2 IU/μL) (Sigma; C5138) was injected steadily over 5 min. Animals in the sham group underwent identical saline injection volume. Post-procedure, a rectal temperature of 37±0.5°C was preserved in recovery period.

Experimental grouping

This paper was split into three sections. 1) Timing of M1-to-M2 transformation: Rats were assigned randomly to the sham group or the IH group (n=5 each). Rats of IH group had an intrastriatum injection of collagenase IV (0.2 U), while those of sham group only injected with saline. 2) Optimal SDDHD Dose: Rats were allocated to sham, IH, low and SDDHD (low, medium, high dose) groups (n=5 each). 3) SDDHD Effects on M2 Microglia: Three groups (sham, IH, and SDDHD-treated, n=5 each) were included.

Drugs

Traditional Chinese herbs were sourced from the Chinese Pharmacy of Zhongshan Hospital, Fudan University. The decocting and preservation methods of traditional Chinese medicine were the same as previously described (Cai *et al*., 2018). SDDHD was prepared as a concentrated solution and administered to rats by gavage twice daily at 9:00 and 16:00. The standard human dosage of Sheng-Di-Da-Huang Decoction was 40g per 60 kg of body weight. Based on the formula: $d_{\text{rat}} = d_{\text{human}} \times 0.7/0.11$, the low, medium and high doses for rats were determined to be 4, 8 and 16 g/kg/day. This dosage selection was also justified by our previous study (Cai *et al*., 2018).

MRI and volume measurement

A 3.0T Siemens MRI with a dedicated rat coil was used. Rats were positioned supine, with scans using T1WI, T2WI, and SWI sequence. After scanning, a contrast agent (0.2mmol/kg) was injected into the tail vein to enhance T1-weighted (CE-T1) imaging for brain edema assessment.

The scan parameters were as followed: T2WI: repetition time (TR): 2210 ms, echo time (TE): 92 ms, field of view (FOV): 64 mm, flip angle 120°, layer thickness 2.0mm, layer number 20, matrix 192x192. T1WI: Pre- and 10-min post-contrast, TR: 400 ms, TE: 12.0 ms, flip angle 90°, FOV 64mm, layer thickness 1.2mm, number of layers 20, matrix 192X192. SWI: three-dimensional gradient echo sequence for paramagnetic sensitivity, TR: 32 ms, TE: 20.0 ms, flip angle 15°, FOV 50mm, layer thickness 1mm, number of layers 20, matrix 320×320. Hematoma volume was derived as the sum of the hematoma area across T2WI slices multiplied by slice thickness.

Neurobehavioral function evaluation

Two observers employed the modified Neurological Severity Score (mNSS) method, as outlined by (Cai *et al*., 2018), to assess neurobehavioral deficits at 1, 3, 7 and 14 days following IH. The mNSS, acting as a composite trial, was exercised for measuring motor, sensory, and balance functions, with scores between 0 (normal) and 13 (maximal deficit).

Western blot analysis

Saline perfusion was performed on the brains prior to decapitation at various time points post-injection. The 1-mm-thick perihematomal brain tissue surrounding the hematoma was harvested. The primary antibodies applied were rabbit anti-Arg1 antibody (1:1000 dilution; Abcam), and rabbit anti-iNOS1 antibody (1:1000 dilution; Abcam). Relative band densities were determined adopting NIH Image J software.

Immunofluorescence Staining

Immunofluorescence procedures involved the fixed rat brain tissues. Specifically, pentobarbital was administered intraperitoneally at 40mg/kg to anesthetize the rats, and 4% paraformaldehyde in 0.1mol/L PBS (pH 7.4) was used for perfusion. After 6-8 hours of post-fixation in 4% paraformaldehyde, the brains were moved to 30% sucrose for 3-4 days at 4°C. Four μm thick coronal sections were obtained through the injection site and 2 mm anterior and posterior to it. Primary antibodies included rabbit anti-Arg1 (1:100 dilutions; Abcam) and rabbit anti-iNOS (1:100 dilution; Abcam). Sections received 30-min incubation with FITC-conjugated anti-rabbit IgG secondary antibody (1:100, Beyotime) at 37°C, then counterstained utilizing DAPI (Beyotime). A light microscope (Olympus/BX51, Tokyo, Japan) was adopted for photographing and observing all sections.

Enzyme-Linked Immunosorbent assay

IL-4 and IL-10 levels in brain tissues were determined with ELISA kit (Elabscience) at different time points after IH. The cytokines were standardized to 100 mg/1 mL of protein in the supernatant for quantification, obeying the manufacturer's guidelines.

Statistical analysis

SPSS version 22.0 (SPSS, Chicago, IL, USA) was exploited for data analysis. The values in this study were presented as mean ± SEM. The Kruskal-Wallis test, with subsequent Mann-Whitney test, was exercised to the neurological deficit scores. Single comparisons were analyzed using the Student t-test and multiple comparisons were assessed using ANOVA with post hoc Bonferroni-Dunn correction. Statistical significance was indicated by a P value of less than 0.05.

RESULTS

Both neurological damage and hematoma volume reached their peak on the third day

Neurological damage and hematoma volume, as appraised via modified Neurological Severity Score (mNSS) (Fig. 1A) and MRI (Fig. 1 B-E), peaked on day 3 post-IH and then gradually declined. T2-weighted and contrast-enhanced T1 (CE-T1) images revealed that hematoma size and brain edema were maximal at this time point.

M1 microglia peaked at 3 days and M2 microglia gradually increased over time

Western blot analysis of perihematomal tissue indicated that M1 marker iNOS increased from day 1, hit a peak on day 3, and subsequently decreased, returning to baseline around day 14. In contrast, the M2 marker Arg1 showed a steady increase over time, suggesting a progressive M1-to-M2 shift (Fig. 2 A-B).

High dose of SDDHD improved neurological function and decresed hematoma

The total neurological function score was 13 points, and the neurological function scores of the four groups of model rats almost all reached the highest on the third day (the most severe neurological deficits) and began to recover gradually thereafter. Rats treated with high-dose SDDHD exhibited significant reductions in neurological deficit scores and hematoma volume on the 7^{th} and 14^{th} days following IH, compared to untreated IH controls ($P<0.05$). Lower doses of SDDHD showed less pronounced effects (Fig. 3A-B).

SDDHD decreased the activation of M1 microglia and increased the activation of M2 microglia after IH

Immunofluorescence and WB functioned to test the M1/M2 markers' expression levels at 3 days to explore the possible mechanism of neuroprotection function of SDDHD on IH. Immunofluorescence (Fig. 4A-B) and Western blot (Fig. 4 C-E) analyses demonstrated reduced iNOS expression and increased Arg1 expression in SDDHD-treated rats compared to the IH group on days 3 and 7 ($P<0.05$), suggesting SDDHD's role in shifting microglial activation from M1 to M2.

SDDHD increased the expression of both IL-4 and IL-10 after IH

ELISA analysis revealed that levels of IL-4 (Fig. 5A) and IL-10 Fig. 5B), both M2-associated cytokines, increased significantly in the SDDHD-treated group at multiple time points compared to the IH group ($P<0.05$). This result indicated enhanced M2 microglial activation and potential anti-inflammatory effects.

DISCUSSION

The primary findings of this study highlight the dynamic transition of microglial phenotypes following IH and the therapeutic potential of SDDHD in modulating this response. Specifically, we observed that M1-type (pro-inflammatory) microglia peaked at day 3 post-IH, followed by a gradual increase in M2-type (anti-inflammatory) microglia. This timing suggests that the M1-to-M2 phenotype switch occurs around day 3, marking a critical window for therapeutic intervention. Treatment with SDDHD not only decreased M1 microglial activity but also promoted M2 activation, accompanied by highly expressed anti-inflammatory markers IL-10 and IL-4. Clinically, these outcomes disclose that SDDHD may function as a promising agent for reducing inflammation and enhancing neuroprotective responses, potentially improving recovery outcomes in patients with IH.

In the brain, microglia take on the primary role of phagocytosis. Microglia, when activated, exhibit two distinct phenotypes: Alternatively activated (M2, anti-inflammatory) or classically activated (M1, pro-inflammatory) (Xiong *et al*., 2016). After IH, microglia activated within a few minutes. Shifts in the markers of M1 and M2 phenotypes over time have been revealed by several studies (Yang *et al*., 2016; Lan, Han, Li, Yang, *et al*., 2017; Taylor *et al*., 2017). Research findings show that IL-1β, TNF-α and IL-6 reach significantly higher levels at 6 hours and start decreasing at 3 days (Lan, Han, Li, Yang, *et al*., 2017). M2 phenotype marker Ym-1 increased at 3 days (Lan, Han, Li, Li, *et al*., 2017) and anti-inflammatory cytokine transforming growth factor-β (TGF-β1), increased from 1 day and remained elevated at 14 days after IH (Taylor *et al*., 2017).

Similar to our study, one study showed that collagenase-mediated IH in mice prompted a switch in microglial phenotype from M1 to M2, starting on day 1 and progressing to day 3 (Lan, Han, Li, *et al*., 2017). The acute inflammatory phase upon IH involved dynamic microglial activation, as observed in this article. Following IH, M1 biomarker iNOS started rising at 1 day, reached their highest point at 3 days, and slowly returned to normal about 14 days. M2 biomarker Arg1 increased over time. IL-10 and IL-4 both increased over time.

Efforts to find effective drugs for IH have never stopped. Several promising drugs have been explored in preclinical studies or clinical trials (Yu *et al*., 2013; Marfia *et al*., 2016; Lan, Han, Li, Li, *et al*., 2017). Sheng-Di-Da-Huang Decoction, containing *Rehmannia glutinosa* and *Rhubarb*, comes from "Wings of the Thousand Gold Pieces Formulary". It can be used for the treatment of various blood syndromes. As our previous study shown, SDDHD demonstrated notable benefits by enhancing neurological

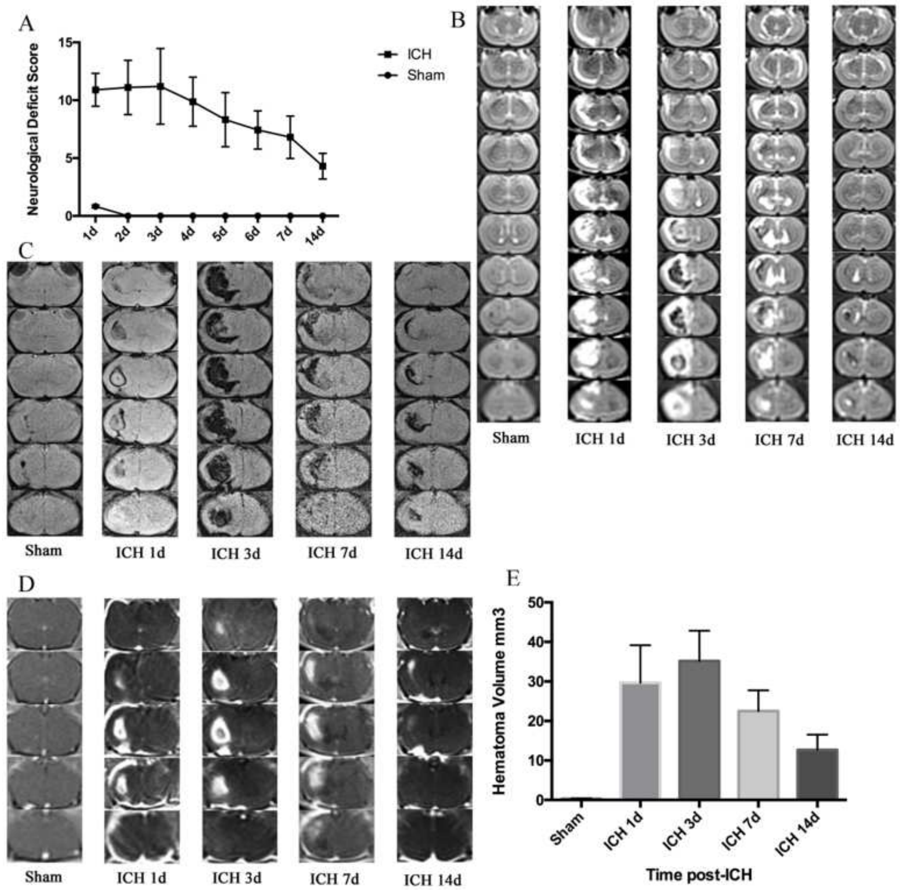

Fig. 1: Peak Neurological Deficit and Hematoma Volume on Day 3 Post-IH. (A). Modified Neurological Severity Score (mNSS) (maximum total score 13). (B). Intracerebral hematoma's representative T2-weighted MR images (coronal sections). (C) Typical SWI images of intracerebral hematoma. (D) Representative CE-T1 images of intracerebral hematoma. (E) Quantification of hematoma volumes from T2-weighted images. Values were displayed by mean ± SEM, n = 5 per group at each time point.

function, minimizing brain water content and Evans blue extra vasation, down regulating TLR4, NF-κB, TNF-α and IL-1β and blocking microglial activation (Cai *et al*., 2018). In this study, we found that SDDHD suppressed the expression of iNOS and increase the expression of Arg-1, IL-4 and IL-10. Combined with the results of the two studies, it can be considered that SDDHD has two-way regulation effect on microglia after IH.

About 70 compounds were isolated from *Rehmannia glutinosa*, mainly iridoids, such as catalpol and dihydrocatalpol. Catalpol has many effects on ischemic stroke. In Sprague Dawley rats with permanent focal cerebral ischemia, catalpol at 10 and 5 mg/kg improves neurobehavioral performance and elevates growth-associated protein 43 expression (Wang J *et al*., 2019). *Rheum officinale* primarily contains anthraquinone derivatives as its active components, comprising aloe emodin, emodin, rhein and chrysophanol. A large number of articles have claimed that rhubarb anthraquinone provides protection against cerebral hemorrhage, with mechanisms likely involving anti-inflammatory, anti-apoptotic and protection of BBB (Zhou X *et al*., 2011; Wang Y *et al*., 2016). However, the relevant active ingredients were not explored in this study, and their specific regulatory mechanisms all need to be confirmed by further experiments.

This study has several limitations. First, it was conducted solely on a rat model, potentially failing to completely replicate the complexity of human IH pathophysiology, which might limit the translatability of our findings to human clinical settings.

Therefore, early-phase clinical trials should be conducted to evaluate the safety, tolerability and preliminary efficacy of SDDHD in human patients with IH. Additionally, the exact molecular mechanisms through which SDDHD modulates microglial phenotype switching remain unclear. Further investigation using techniques like Western blotting or qPCR to explore pathways such as TLR4/NF-κB and PI3K/AKT is needed to clarify its effects. Furthermore, while SDDHD improved neurobehavioral outcomes, the long-term effects and safety of this treatment need to be assessed in future studies.

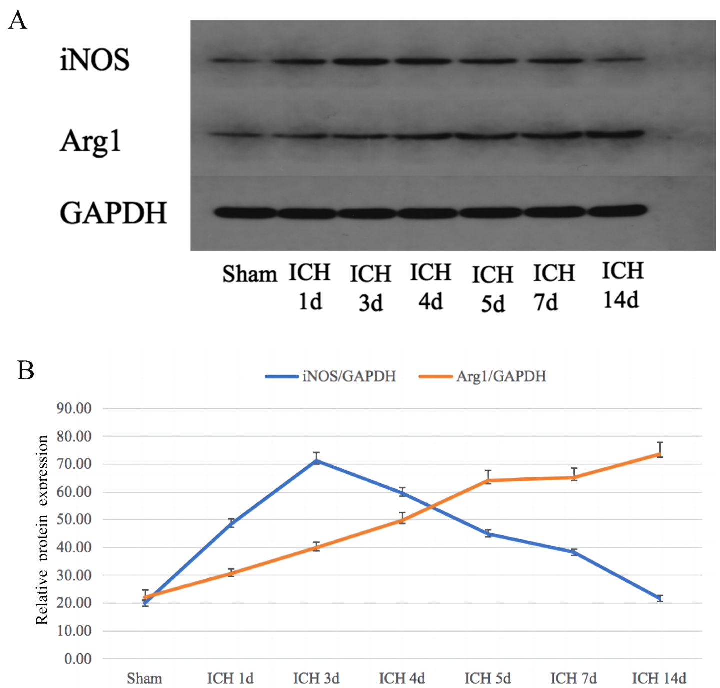

Fig. 2: Detection of iNOS and Arg1 in the hemorrhagic area. (A) Western blot bands for Arg1 and iNOS at every time interval. (B) Quantitative outcomes of Arg1 and iNOS relative to GAPDH. Data were exhibited via mean ± SEM, n = 5 rats per group.

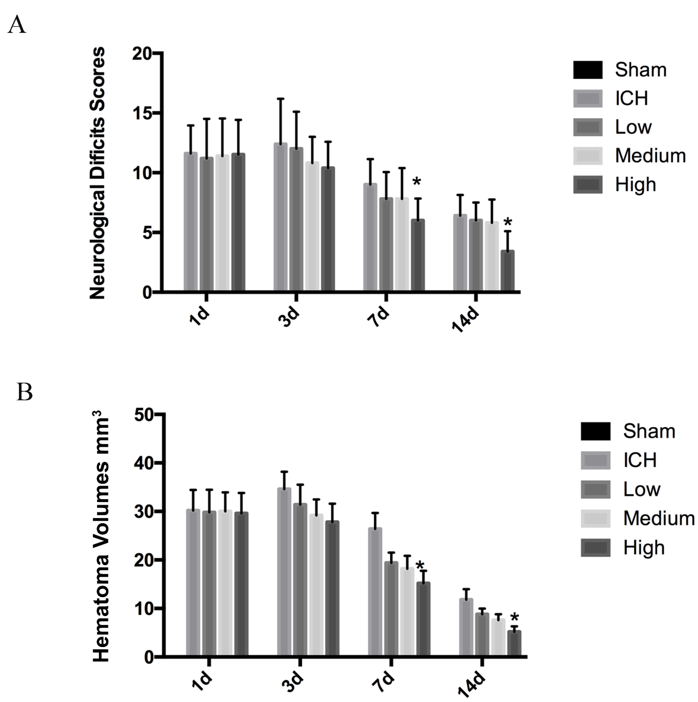

Fig. 3: Effects of SDDHD dosage on neurological function and hematoma volume on rats with intracerebral hemorrhage. (A) Rats' neurological deficit scores (maximum score of 13) after collagenase injection. (B) Hematoma volume outcomes. Data were represented by mean ± SEM, with n = 5 rats in each group. *P<0.05 vs. IH group.

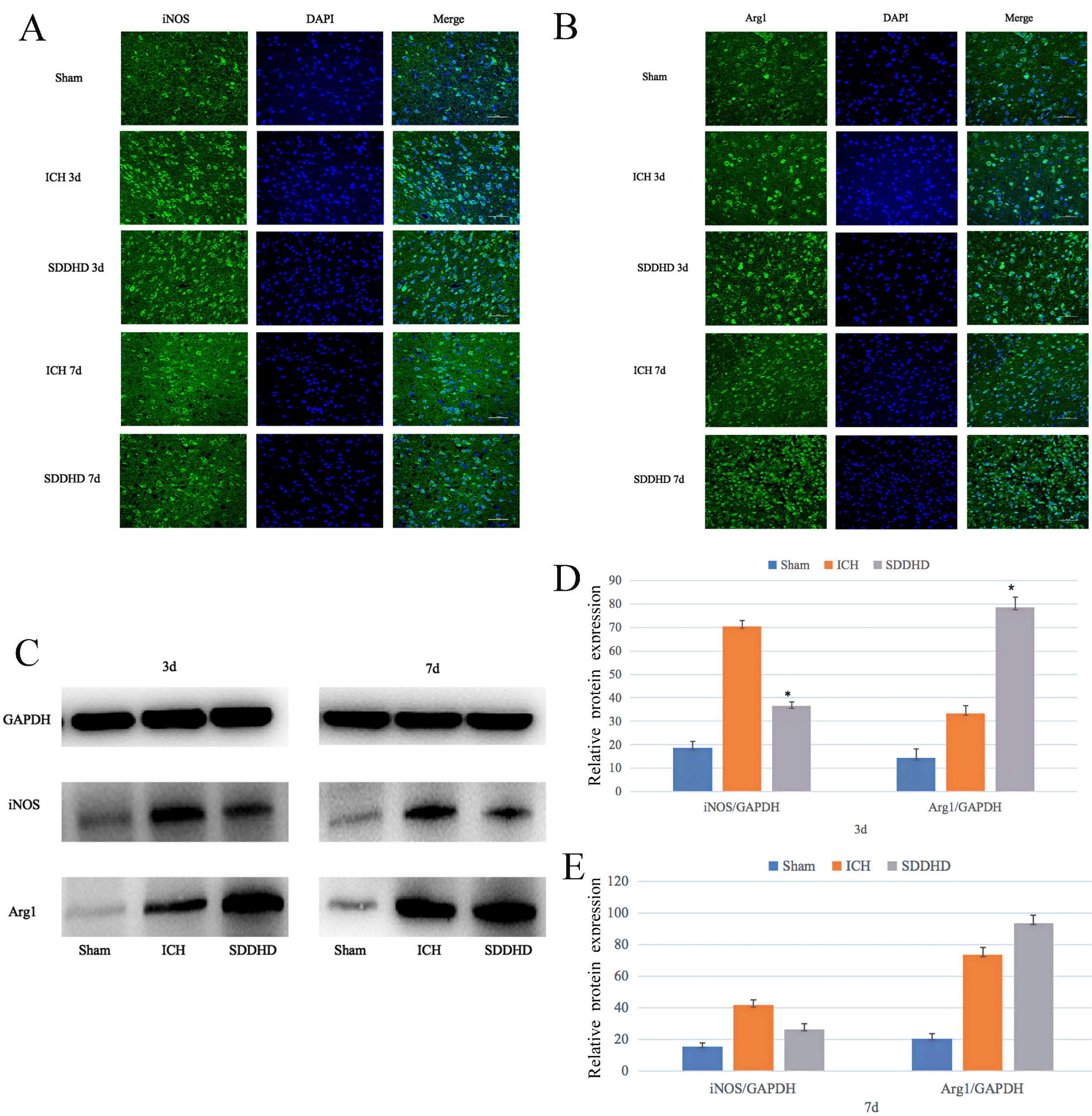

Fig. 4: SDDHD's impact on M1 and M2 microglial activation markers (A). Immunofluorescence images of iNOS (green) in sham group and the perihematomal region at days 3 and 7 upon IH, × 200 magnified. (B) Immunofluorescence images of Arg1 (green) in the perihematomal area and sham group at 3 and 7 days after IH, × 200 magnified. (C) Western blot bands of iNOS and Arg1 at 3 and 7 days. (D-E) Quantification of iNOS/Arg1 relative to GAPDH at 3 and 7 days. Mean ± SEM was utilized for data expression, with each group consisting of 5 rats (n = 5). *$P<0.05$ vs. IH group.

In summary, while our findings suggest that SDDHD holds promise as a therapeutic intervention for IH, further research, including clinical trials and molecular mechanistic studies, is needed to fully understand its therapeutic potential and long-term safety.

CONCLUSION

SDDHD exerts a bidirectional regulatory effect on microglia after IH, both suppressing M1-type microglial activation and promoting M2-type transformation. These effects appear to improve neurological function and reduce inflammation and brain edema, highlighting SDDHD's potential as a novel therapeutic approach for IH. Translating these results into clinical applications and uncovering the mechanisms of SDDHD's role in microglial modulation should be key focuses of future research.

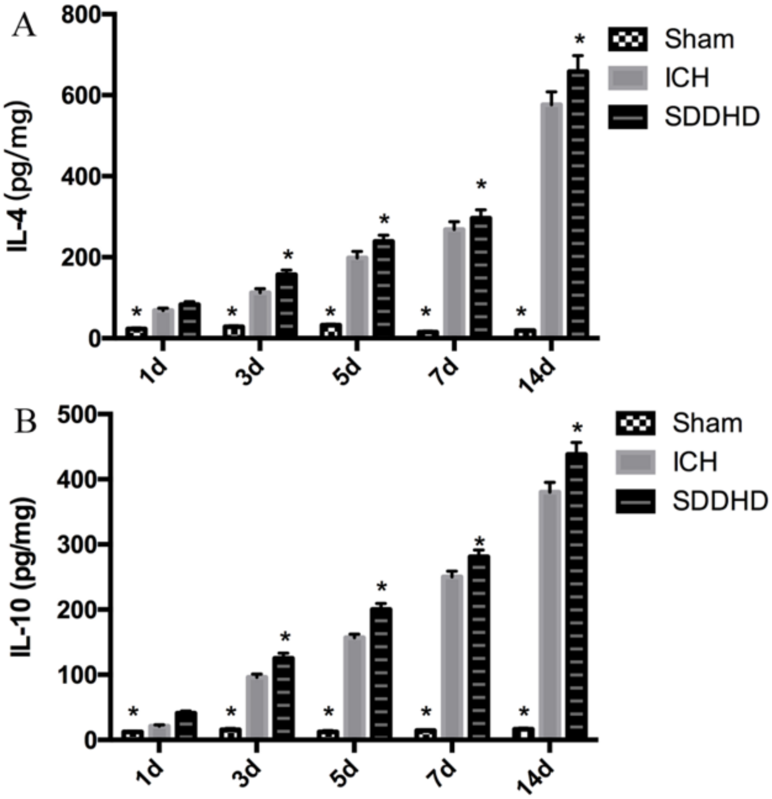

Fig. 5: SDDHD enhances IL-4 and IL-10 expression post-IH. (A) IL-4 and (B) IL-10 concentrations at various time intervals. Data were exhibited by mean ± SEM, with five rats in each group (n = 5). *P<0.05 vs. IH group.

Acknowledgement
Not applicable.

Authors' contributions
Study concept and design: MC, DC; Analysis and interpretation of data: JZ, ML, LY, JX; Data Acquisition: FY, WZ, XB, DQ, WZ; Drafting of the manuscript: MC; Critical revision of the manuscript for important intellectual content: MC, DC; Statistical analysis: LX, YX; Funding acquisition: DC; Study supervision: all authors; all authors have read and approved the manuscript.

Funding
This study was supported by the National Natural Science Foundation of China (81703849 and 81503555), the Shanghai Key Clinical Specialty Project of Emergency Medicine (Grant No. shslczdzk04403) and the Outstanding Youth Fund Project of Zhongshan Hospital, Fudan University (Grant No. 2019ZSYQ33).

Data availability statement
The datasets generated during and/or analysed during the current study are available from the corresponding author on reasonable request.

Ethical approval
Approval for the trial was granted by the Ethics Committee of Fudan University (No. 201703849), with animal procedures following the guidance of the Animal Care and Use Committee (ACUC) of Fudan University and National Institutes of Health Guide for the Care and Use of Laboratory Animals.

Conflict of interest
The authors declare that there are no conflicts of interest regarding the publication of this paper.

REFERENCES

Cai M, Yu Z, Zhang W, Yang L, Xiang J, Zhang J, Zhang Z, Wu T, Li X, Fu M, Bao X, Yu X and Cai D (2018). Sheng-Di-Da-Huang decoction inhibited inflammation expressed in microglia after intracerebral hemorrhage in rats.: *eCAM*, 6470534.

Chowdhury S and Trivedi AK (2023). Origin, production and molecular determinants of macrophages for their therapeutic targeting. *Cell Biol. Int.*, **47**(1): 15-29.

Fogelholm R, Murros K, Rissanen A, Avikainen S. (2005). Long term survival after primary intracerebral haemorrhage: A retrospective population based study. *J. Neurol. Neurosurg. Psychiatry*, **76**(11): 1534-1538.

Kanazawa M, Ninomiya I, Hatakeyama M, Takahashi T and Shimohata T (2017). Microglia and monocytes/ macrophages polarization reveal novel therapeutic mechanism against stroke. *Int. J. Mol. Sci.*, **18**(10): 2135.

Lan X, Han X, Li Q, Li Q, Gao Y, Cheng T, Wan J, Zhu W and Wang J (2017). Pinocembrin protects hemorrhagic brain primarily by inhibiting toll-like receptor 4 and reducing M1 phenotype microglia. *Brain Behav. Immun.*, **61**: 326-339.

Lan X, Han X, Li Q, Yang QW and Wang J (2017). Modulators of microglial activation and polarization after intracerebral haemorrhage. *Nat. Rev. Neurol.*, **13**(7): 420-433.

Marfia G, Navone SE, Hadi LA, Paroni M, Berno V, Beretta M, Gualtierotti R, Ingegnoli F, Levi V, Miozzo M, Geginat J, Fassina L, Rampini P, Tremolada C, Riboni L and Campanella R (2016). The adipose mesenchymal stem cell secretome inhibits inflammatory responses of microglia: Evidence for an involvement of sphingosine-1-phosphate signalling. *Stem. Cells Dev.*, **25**(14): 1095-1107.

Mracsko E and Veltkamp R (2014). Neuroinflammation after intracerebral hemorrhage. *Front Cell Neurosci.*, **8**: 388.

O'Carroll CB, Brown BL and Freeman WD (2021). Intracerebral hemorrhage: A common yet disproportionately deadly stroke subtype. *Mayo Clinic proceedings*, **96**(6): 1639-1654.

Puy L, Parry-Jones AR, Sandset EC, Dowlatshahi D, Ziai W and Cordonnier C (2023). Intracerebral haemorrhage. *Nat. Rev. Dis. Primers,* **9**(1): 14.

Taylor RA, Chang CF, Goods BA, Hammond MD, Mac Grory B, Ai Y, Steinschneider AF, Renfroe SC, Askenase MH, McCullough LD, Kasner SE, Mullen MT, Hafler DA, Love JC and Sansing LH (2017). TGF-beta1 modulates microglial phenotype and promotes recovery after intracerebral hemorrhage. *J. Clin. Invest.*, **127**(1): 280-292.

van Asch CJ, Luitse MJ, Rinkel GJ, van der Tweel I, Algra A and Klijn CJ (2010). Incidence, case fatality, and functional outcome of intracerebral haemorrhage over time, according to age, sex and ethnic origin: A systematic review and meta-analysis. *Lancet Neurol.*, **9**(2): 167-176.

Wang J, Wan D, Wan G, Wang J, Zhang J and Zhu H (2019). Catalpol induces cell activity to promote axonal regeneration via the PI3K/AKT/mTOR pathway *in vivo* and *in vitro* stroke model. *Ann. Transl. Med.*, **7**(23): 756.

Wang Y, Peng F, Xie G, Chen ZQ, Li HG, Tang T and Luo JK (2016). Rhubarb attenuates blood-brain barrier disruption via increased zonula occludens-1 expression in a rat model of intracerebral hemorrhage. *Exp. Ther. Med.*, **12**(1): 250-256.

Wu S, Wu B, Liu M, Chen Z, Wang W, Anderson CS, Sandercock P, Wang Y, Huang Y, Cui L, Pu C, Jia J, Zhang T, Liu X, Zhang S, Xie P, Fan D, Ji X, Wong KL, Wang L. China stroke study collaboration. (2019). stroke in China: Advances and challenges in epidemiology, prevention and management. *Lancet Neurol*, **18**(4): 394-405.

Xiong XY, Liu L and Yang QW (2016). Functions and mechanisms of microglia/macrophages in neuroinflammation and neurogenesis after stroke. *Prog. Neurobiol.*, **142**: 23-44.

Yang J, Ding S, Huang W, Hu J, Huang S, Zhang Y and Zhuge Q (2016). Interleukin-4 ameliorates the functional recovery of intracerebral hemorrhage through the alternative activation of microglia/macrophage. *Front Neurosci.*, **10**: 61.

Yu Z, Tang L, Chen L, Li J, Wu W and Hu C (2013). Erythropoietin reduces brain injury after intracerebral hemorrhagic stroke in rats. *Mol. Med. Rep.*, **8**(5): 1315-1322.

Zhao H, Garton T, Keep RF, Hua Y and Xi G (2015). Microglia/macrophage polarization after experimental intracerebral hemorrhage. *Transl Stroke Res.*, **6**(6): 407-409.

Zhou M, Wang H, Zeng X, Yin P, Zhu J, Chen W, Li X, Wang L, Wang L, Liu Y, Liu J, Zhang M, Qi J, Yu S, Afshin A, Gakidou E, Glenn S, Krish VS, Miller-Petrie MK, Mountjoy-Venning WC and Liang X (2019). Mortality, morbidity and risk factors in China and its provinces, 1990-2017: A systematic analysis for the global burden of disease study 2017. *Lancet*, **394**(10204): 1145-1158.

Zhou X, Wang L, Wang M, Xu L, Yu L, Fang T and Wu M (2011). Emodin-induced microglial apoptosis is associated with TRB3 induction. *Immunopharmacol Immunotoxicol.*, **33**(4): 594-602.